NTIA Report 20-548

3.45–3.65 GHz Spectrum Occupancy from Long-Term Measurements in 2018 and 2019 at Four Coastal Sites

Michael Cotton
Linh Vu
Bradley Eales
Adam Hicks

report series

U.S. DEPARTMENT OF COMMERCE • National Telecommunications and Information Administration

NTIA Report 20-548

3.45–3.65 GHz Spectrum Occupancy from Long-Term Measurements in 2018 and 2019 at Four Coastal Sites

Michael Cotton
Linh Vu
Bradley Eales
Adam Hicks

U.S. DEPARTMENT OF COMMERCE

Douglas Kinkoph, Associate Administrator, performing the delegated duties of the Assistant Secretary of Commerce for Communications and Information

April 2020

DISCLAIMER

Certain commercial equipment and materials are identified in this report to specify adequately the technical aspects of the reported results. In no case does such identification imply recommendation or endorsement by the National Telecommunications and Information Administration, nor does it imply that the material or equipment identified is the best available for this purpose.

CONTENTS

FIGURES

TABLES

ABBREVIATIONS AND ACRONYMS

β	Band occupancy
ξ_{jk}	Measured sample function of channel occupancy
APD	Amplitude probability distribution
AS	Astoria, OR
BPF	Bandpass filter
CBRS	Citizen Broadband Radio Service
dB	Decibel; logarithmic unit used to expressed the ratio between two values
dBi	Decibel relative to isotropic radiator
dBm	Power ratio in decibels of measured power referenced to one milliwatt
DFT	Discrete Fourier Transform
$\mathcal{E}\{\cdot\}$	Expected value operator
ENBW	Equivalent noise bandwidth
ENR	Excess noise ratio
ESC	Environmental Sensing Capability
FCC	Federal Communications Commission
FISMA	Federal Information Security Modernization Act
GHz	Gigahertz (10^9 Hertz)
ITS	Institute for Telecommunication Sciences
kHz	Kilohertz (10^3 Hertz)
LNA	Low noise amplifier
M4	Maximum, mean, median, and minimum
M_β	Mean band occupancy
MHz	Megahertz (10^6 Hertz)
MSps	Million samples per second
N	Number of observations or scans
N_c	Number of channels or frequencies
NF	Norfolk, VA
NTIA	National Telecommunications and Information Administration
OL	Overload
OOB	Out-of-band
$\hat{p}$	Channel occupancy estimate

P_n	Mean system noise power or RMS-detected system noise
P_R	Mean power received
$\wp\{\cdot\}$	Probability operator
PS	Preselector
RF	Radio frequency
RMS	Root mean square
SD	San Diego, CA
SF	San Francisco, CA
SigAn	Signal analyzer
SMS	Spectrum Monitoring System (NTIA FISMA Major Application)
SPN-43	Maritime air-marshaling radar that operates in the upper S-band

3.45−3.65 GHZ SPECTRUM OCCUPANCY FROM LONG-TERM MEASUREMENTS IN 2018 AND 2019 AT FOUR COASTAL SITES

Michael Cotton, Linh Vu, Bradley Eales, and Adam Hicks[1]

This report presents spectrum occupancy results for 3.45–3.55 GHz and for 3.55−3.65 GHz at sensor sites near San Diego CA (SD), Norfolk VA (NF), San Francisco CA (SF), and Astoria OR (AS). Sensors operated at the following {start date, end date, 2018 reliability, 2019 reliability}: SD {05/17, 09/19, 53.2%, 35.4%}, NF {05/17, 12/19, 61.7%, 74.2%}, SF {11/17, 12/19, 86.4%, 28.7%}, AS {05/18, 09/19, 46.7%, 100.0%}. The acquired data was processed to monthly and yearly mean band occupancy estimates. At ports with high military presence,{2018, 2019} yearly mean band occupancy levels were {25.0, 21.9}% in SD and {9.0, 9.9}% in NF for 3.45−3.55 GHz and {14.7, 13.3}% in SD and {13.6, 22.4}% in NF for 3.55−3.65 GHz. At ports with low military presence, {2018, 2019} yearly mean band occupancy levels were {1.0, 0.3}% in SF and {0.3, 0.2}% in AS for 3.45−3.55 GHz and {0.1, 0.0}% in SF and {0.0, 0.1}% in AS for 3.55−3.65 GHz.

Keywords: 3450-3550 MHz, 3550-3650 MHz, Citizen Broadband Radio Service (CBRS), radar, spectrum monitoring, spectrum occupancy, spectrum sharing

1. INTRODUCTION

The purpose of this report is to provide spectrum occupancy results for 3.45−3.55 GHz and 3.55−3.65 GHz from radio-frequency (RF) sensors installed near San Diego CA (SD), Norfolk VA (NF), San Francisco CA (SF), and Astoria OR (AS) acquiring data mostly continuously from January 2018 to December 2019. This data is relevant to NTIA's technical study on the feasibility of sharing federal spectrum with future commercial operations in the 3450−3550 MHz band [1] and to the Citizen Broadband Radio Service (CBRS) [2]. Background information on U.S. spectrum repurposing in this frequency range can be found in NTIA's Annual Report on the Status of Spectrum Repurposing (2019) [3].

This report is structured as follows: Section 2 describes measurement strategy; Section 3 describes data processing; Section 4 provides long-term results; Section 5 provides a summary; Appendix A gives example metadata that specifies hardware and defines algorithm parameters; Appendix B gives sensor configuration management parameters with notes on sensor install/uninstall dates, configuration changes, and sensor reliability; and Appendix C provides information from sensors by month in tabular form.

[1] The authors are with the Institute for Telecommunication Sciences, National Telecommunications and Information Administration, U.S. Department of Commerce, Boulder, CO 80305.

2. MEASUREMENT STRATEGY

This section describes sensor hardware, software, and installations. The goal of the measurement strategy was to perform continuous (24/7) long-term measurements in order to provide factual occupancy information for 3.45−3.65 GHz emitters at and around the four locations. There are important ground-based, shipborne, and airborne government systems that operate in this frequency range; see [1], [4] for assignment parameters and locations. The sensor design (e.g., antenna selection, detection scheme) and installation (e.g., location, antenna configuration) are designed for detecting the SPN-43 air-marshalling radar that operates at 3.5−3.65 GHz and is a primary emitter in this band. This approach is not necessarily optimal for detecting all 3.5 GHz ground-based, shipborne, and airborne systems. Further, the sensors were not designed to meet nor tested against CBRS ESC requirements [5] [6].

2.1 System Description

Figure 1 provides a block diagram of the sensor, which includes an antenna, preselector (PS), signal analyzer (SigAn), and measurement controller with a computer. The antenna was a broadband slant-polarized omnidirectional antenna with a nominal gain of 0 dBi and an elevation beamwidth of 50−80 degrees. The software-controllable PS provided: (a) signal source for self-calibrations, (b) preselection for low-noise-figure measurements in up to two bands, and (c) bypass RF path for measurements at the full-frequency range and noise figure of the antenna plus SigAn. The PS was configured with preselection for 3.45−3.65 GHz. The software-controllable SigAn provided: (a) frequency range of 0.02−6 GHz, (b) maximum sample rate of 28 million samples per second (MSps), (c) root mean square (RMS) and peak detection for 5 second integration (or dwell) times, and (d) front-end attenuation up to 30 dB in 1 dB steps.

Prior to installation, the sensors were calibrated at the research and engineering laboratory of the National Telecommunications and Information Administration, the Institute for Telecommunication Sciences (NTIA/ITS). Specifically, y-factor calibrations (using a noise source with a calibrated excess noise ratio (ENR)) were performed to measure noise figure and gain for each of the SigAn attenuation settings. The resulting calibration tables were loaded into the sensors to support dynamic-attenuation measurements. Table 1 provides sensor subsystem parameters and laboratory calibration results. Only calibration results for 3 dB SigAn attenuation are shown in Table 1.

After installation, the software-controlled measurement system was designed to cycle through the following schedule of actions: (1) y-factor calibration every six hours and (2) peak-detection scan from 3.45 to 3.65 GHz continuously.

Peak-detected scan data (at 0.9625 MHz equivalent noise bandwidth) was acquired via 64-bin discrete Fourier transforms (DFT) on a digitized complex-baseband signal sampled at 28 MSps with a Gaussian-Top window applied. Only the middle 20 MHz of the DFT was kept to avoid edge effects of the SigAn anti-aliasing filter. A five-second dwell time was chosen to ensure that at least one SPN-43 antenna rotation was captured during each detection interval [7]. Hence, 50 seconds was required to scan across the 200 MHz.

The sensor software also applied dynamic attenuation, i.e., SigAn attenuation was added when a strong signal caused overload (OL). Adding SigAn attenuation can increase the noise figure. Hence, the noise figure for the SigAn attenuation applied in a given measurement was pulled from the onboard calibration table and included in metadata packaged with the measured data.

Appendix A provides example metadata from the San Diego sensor that defines the sensor hardware, configuration, and algorithms. Metadata and data for all sensors were packaged according to the gnuradio Signal Metadata Format Specification (SigMF) [8] and the SigMF-NS-NTIA extension [9]—i.e., NTIA's open data format for recorded signal datasets.

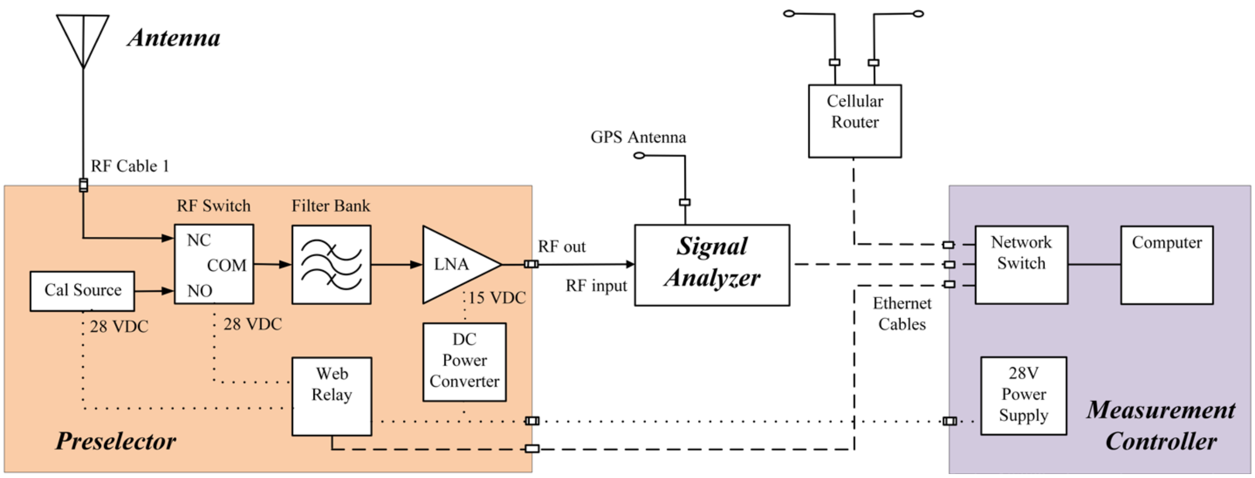

Figure 1. Sensor block diagram.

Table 1. Sensor parameters and laboratory calibration data

Subsystem	Parameter	SD	NF	SF	AS
Antenna	Frequency Range [GHz]	2–6	2–6	2–6	2 - 6
	Gain [dBi] *	0.0	0.0	0.0	0.0
	Cable 1 Loss [dB] *	1.0	3.2	0.7	1.8
Preselector	Cal Source ENR [dB] *	14.5	14.3	14.5	14.9
	BPF Freq Range [GHz]	3.43–3.67	3.43–3.67	3.43–3.67	3.43–3.67
	LNA Gain [dB] *	30.6	32.7	32.9	32.1
	LNA Noise Figure [dB] *	2.8	2.2	2.6	2.1
	LNA Max Output [dBm] *	27.4	27.9	27.6	27.8
Signal Analyzer	Frequency Range [GHz]	0.02–6	0.02–6	0.02–6	0.02–6
	Max Sample Rate [MSps]	28.0	28.0	28.0	28.0
	Max Attenuation [dB]	30.0	30.0	30.0	30.0
Sensor Calibration	Gain [dB] *, **	26.1	26.6	27.3	27.7
	Noise Figure [dB] *, **	8.4	7.9	7.6	7.1

* Specified for 3.5 GHz
** Specified for 3 dB SigAn attenuation

2.2 Installations

SD and NF were chosen as measurement sites because of their close proximity to naval bases and operations. SF and AS were selected as active ports with relatively less military presence. All measurement sites had approximately 180-degree field of view over the ocean.

The sensors were operated as remote equipment without direct and immediate engineering or technician support. Appendix B provides a sensor configuration management log, brief descriptions of installation procedures, and percentages of times the sensors were operational (i.e., reliability) by month. Sensor downtimes were variable and sometimes long, especially when travel to a remote site was required. Table 2 provides a summary of sensor operations for 2018 and 2019 with date ranges, number of observations (N), and reliability. Figure 2 provides pictures from each site during installation.

Table 2. Sensor operation date ranges, number of observations, and reliability [%].

Sensor	Start Date	End Date	2018		2019	
			N	Reliability	N	Reliability
SD	05/12/2017	09/18/2019	251,668	53.2	128,630	35.4
NF	05/24/2017	12/31/2019	317,129	61.7	384,090	74.2
SF	11/14/2017	12/31/2019	453,199	86.4	149,794	28.7
AS	05/31/2018	09/17/2019	164,701	46.7	370,161	100.0

(a) (b) (c) (d)

Figure 2. Pictures of installation sites: (a) ITS engineer in SD, (b) measurement controller and PS at NF, (c) SF equipment rack, (d) AS antenna and PS mounted on tower.

3. DATA PROCESSING

This section describes the data processing to calculate occupancy. A more rigorous discussion is given in [7].

3.1 Occupancy

Figure 3 depicts detected signal power versus time at a given frequency. Occupancy is a threshold exceedance statistic. The multiple thresholds (L_i) shown in Figure 3 illustrate that a lower threshold results in larger occupancy, i.e., more sensitive sensors see signals at lower power levels. When measurements are used to estimate occupancy, it is important have system noise characterized.

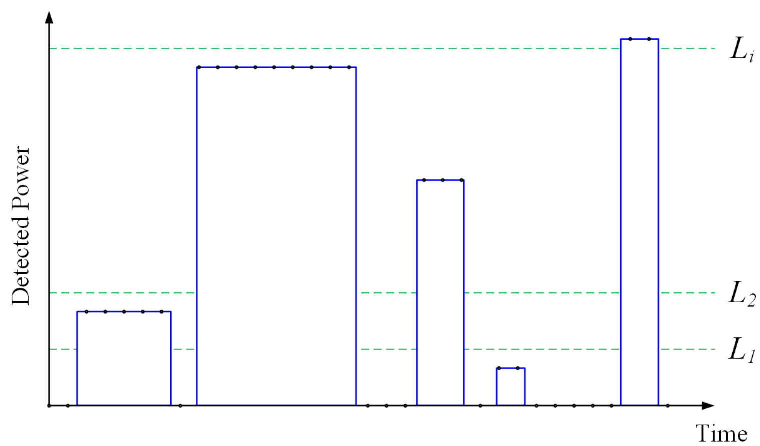

Figure 3. Detected signal power versus time at a given frequency.

Assuming that the received signal power at a given frequency is a random process (which is identified, along with random variables, by bold font), the two-state random process is defined as

$$\boldsymbol{X}(t) = \begin{cases} 1 & \text{if signal power exceeds threshold } L \\ 0 & \text{else} \end{cases} , \tag{1}$$

and channel occupancy as

$$p(t) = \wp\{\boldsymbol{X}(t) = 1\} . \tag{2}$$

In general, to estimate channel occupancy, N observations of random process $\boldsymbol{X}(t)$ are made over time interval T and the time average is calculated as

$$\hat{p}_k = \frac{1}{N} \sum_{j=1}^{N} \xi_{jk} , \tag{3}$$

where ξ_{jk} are the observations, j is the time index, and k is the frequency index.

A useful metric in spectrum management is band occupancy, which is intuitively defined at any given time as the fraction of frequencies (or channels) with a detected signal level that exceeds a predetermined threshold. This is depicted in Figure 4.

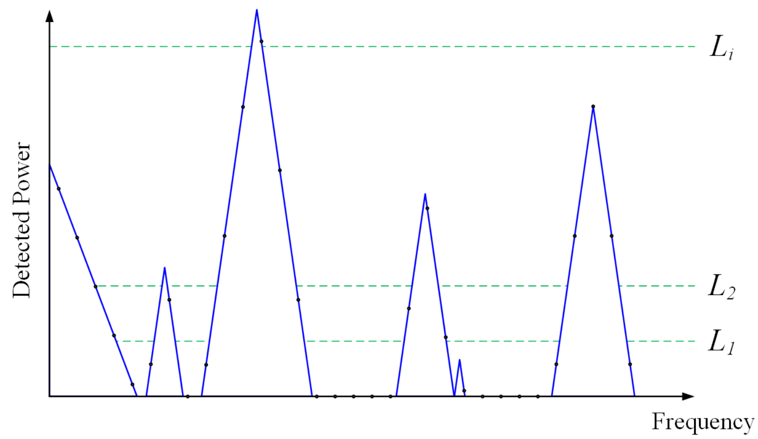

Figure 4. Detected signal power versus frequency at a given time.

Measured band occupancy at a given time is calculated as

$$\beta_j = \frac{1}{N_c}\sum_{k=1}^{N_c} \xi_{jk} \ , \tag{4}$$

where N_c is the number of channels sampled. Further, N measurements of band occupancy are acquired and the mean band occupancy is calculated as

$$M_\beta = \frac{1}{N}\sum_{j=1}^{N} \beta_j = \frac{1}{N_c}\sum_{k=1}^{N_c} \hat{p}_k \ . \tag{5}$$

3.2 Observations and Example Calculations - San Diego, August 2018

This subsection provides illustrations of data acquired near SD in August, 2018. Figure 5 depicts a spectrogram with N = 35,667 scans. The reference point for peak-detected signal power is at the antenna terminal. The gray-shaded areas indicate sensor downtime. The white areas indicate time/frequency where no signals were observed above -88 dBm.

Figure 6 provides maximum, median, mean, and minimum (M4) statistics of the peak-detected signals at each frequency acquired from the SD sensor in August 2018. M4 plots are a useful presentation because one can distinguish signal characteristics, especially in the maximum curves. The black dashed horizontal line indicates sensor OL threshold—as noted in subsection 2.1, SigAn attenuation is triggered in these cases to preserve system linearity.

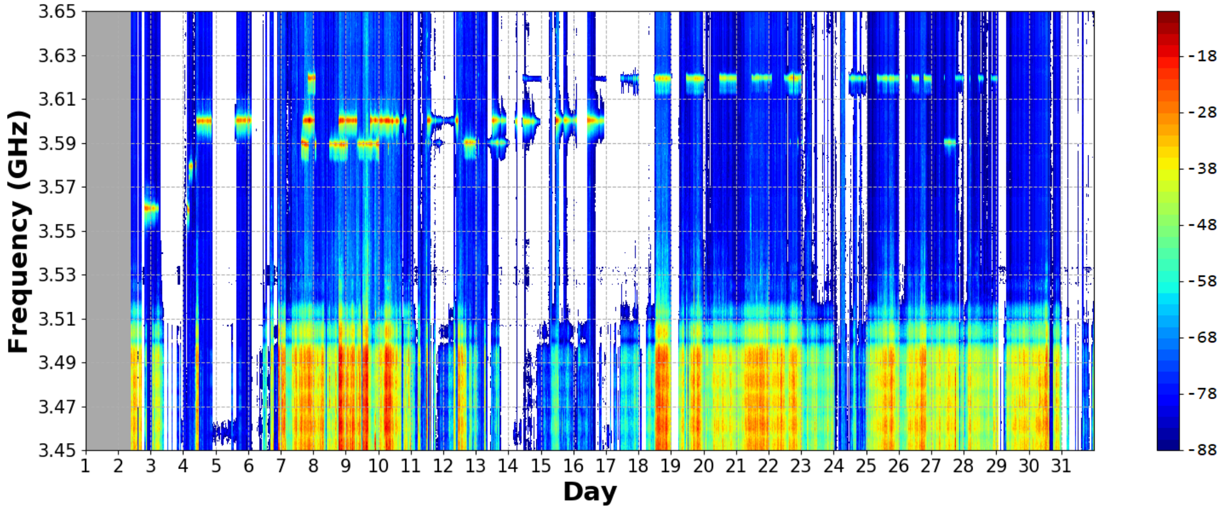

Figure 5. Spectrogram of peak-detected measurements [dBm] from San Diego in August 2018.

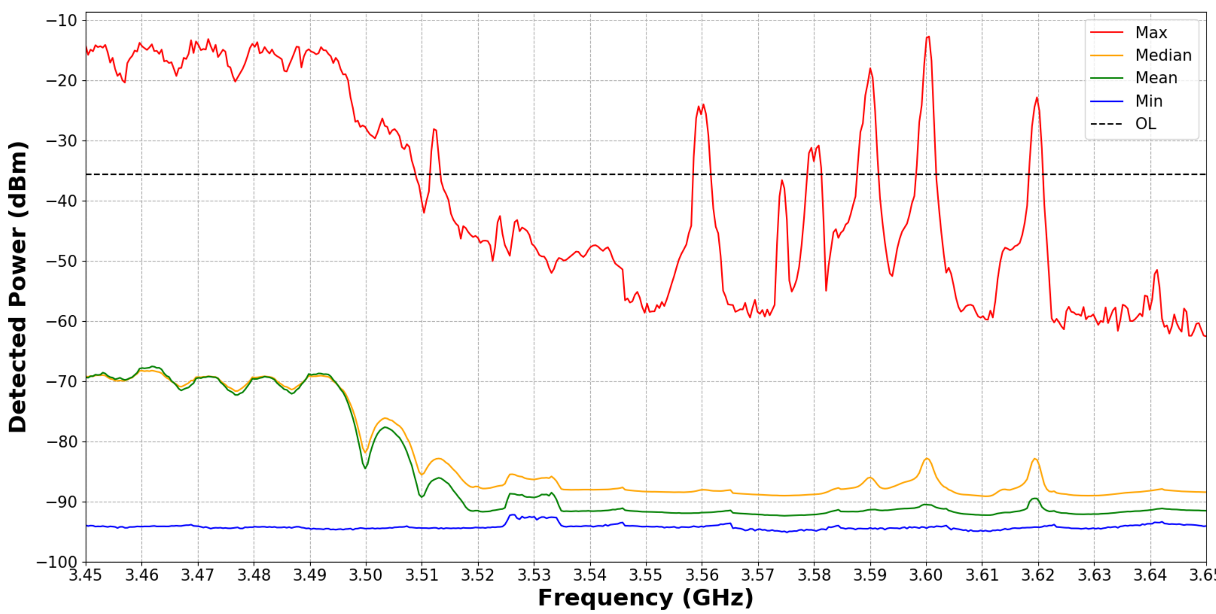

Figure 6. M4 statistics of peak-detected measurements from San Diego in August 2018.

Observe in Figures 5 and/or 6: (1) intermittent SPN-43 signals at 3.56 GHz, 3.58 GHz, 3.59 GHz, 3.60 GHz, and 3.62 GHz; (2) intermittent Radar 3 signal below 3.5 GHz; and (3) out-of-band (OOB) Radar 3 signals above 3.5 GHz [10].

Figure 7 gives amplitude probability distributions (APDs) of peak-detected data acquired at 3.45−3.55 GHz and 3.55−3.65 GHz from the SD sensor in August 2018. The lower and upper 100 MHz of the measurement span were intentionally focused upon to align with portions of spectrum bands under examination pursuant to the MOBILE NOW Act of 2018 [11] and the CBRS band, respectively.

APDs are the complement to cumulative distribution functions in that they offer exceedance probabilities. APDs are plotted on Rayleigh paper, which offers advantages when observing signals in Gaussian noise.

The blue and yellow curves in Figure 7 give the percentage of the approximately 8.2 million (NxN_c) peak-detected measurements (x-axis) that exceeded a specified threshold (y-axis), which is equivalent to $\sum_{jk} \xi_{jk}/(NN_c) = M_\beta$. Hence, the grey circles specify the mean band occupancies M_β = {42.7, 29.0, 19.4}% in 3.45−3.55 GHz in contrast to M_β = {13.3, 2.2, 1.0}% for 3.55−3.65 GHz for thresholds L = {-80, -70, -60} dBm. This set of thresholds were chosen to demonstrate M_β dependency on L. In Section 4, a common threshold (based on local calibration data) is selected to allow for comparison of long-term occupancy statistics between sensors.

The green and red curves in Figure 7 give the percentage of N = 35,667 scan maximums (x-axis) that exceed a specified threshold (y-axis). The dashed black line illustrates sensor OL level (at default SigAn attenuation). As indicated by black circles, 3.45−3.55 GHz scans exceeded the OL level 10.3% of the time. In comparison, 3.55−3.65 GHz scans exceeded OL 4.7% of the time and 3.45−3.65 GHz scans exceeded OL 12.8% of the time (calculated separately).

In a similar process, APDs were generated for the full year to estimate yearly mean band occupancy. The following section provides yearly and monthly mean band occupancy estimates for both 2018 and 2019. It is worth noting that monthly and yearly band occupancy estimates were calculated from times when the sensors were actively monitoring. Uncertainty analysis to derive confidence intervals for mean band occupancy estimates, similar to that performed for channel occupancy estimates in [7], is the subject of further study and outside the scope of this report.

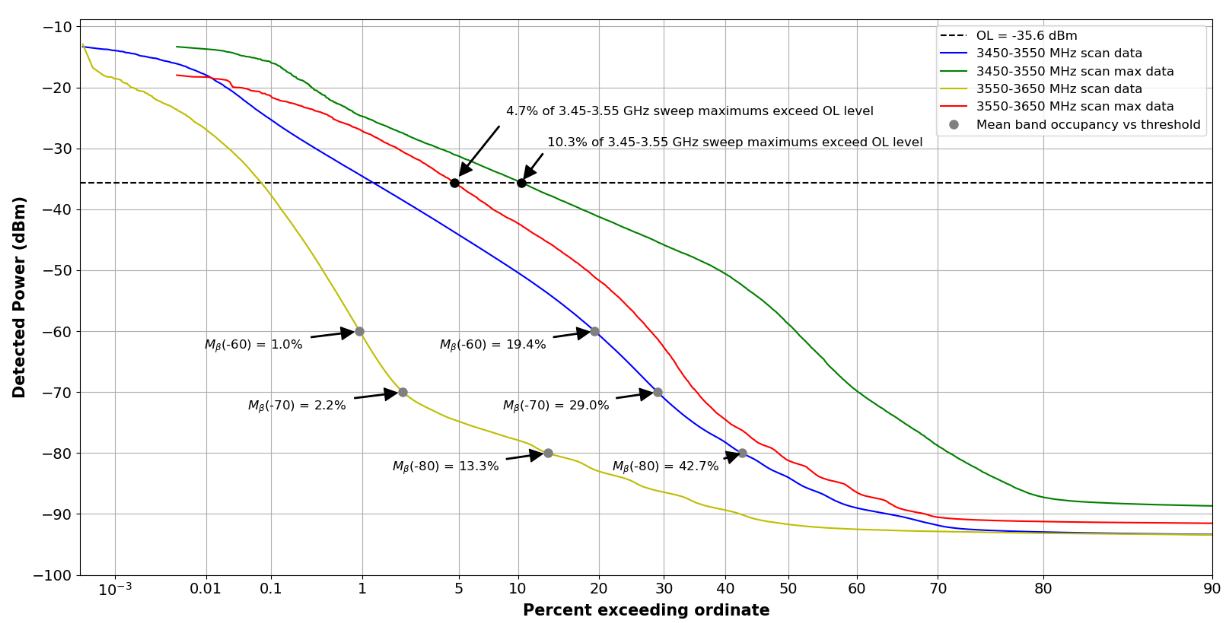

Figure 7. Mean occupancy estimates from APDs of peak-detected measurements at 3.45−3.55 GHz and 3.55−3.65 GHz from San Diego in August 2018.

4. LONG-TERM RESULTS

In this section, long-term mean band occupancy statistics are provided. Appendix C complements this section by providing information from sensors by month in tabular form.

4.1 Calibration Data

Figure 8 illustrates peak-detected system noise levels (referenced at antenna terminal) measured at 3.55 GHz during self-calibrations. Note the trend to increased noise figures with time. Pragmatically, system noise should not contribute to the occupancy estimate. Given this data, a common threshold of L = -88 dBm was selected for occupancy calculations to allow for comparisons.

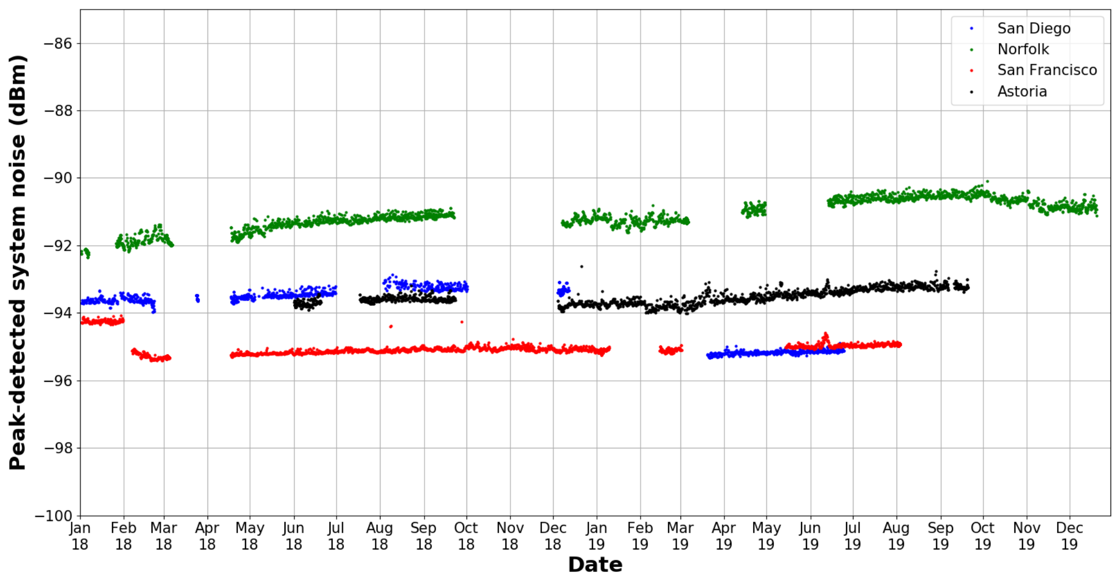

Figure 8. Peak-detected system noise levels measured during calibrations.

4.2 Yearly and Monthly Mean Band Occupancy

Table 3 provides yearly mean band occupancy estimates. Note that there were significant time intervals when measurements were not performed. In some cases, zero measurements for a month or more. In San Diego, for example, zero measurements were performed July 2018, October–November 2018, January–February 2019, and July 2019–December 2019.

Table 3. Yearly mean band occupancy M_β (%) for threshold L = -88 dBm

Frequency Range	**San Diego**		**Norfolk**		**San Francisco**		**Astoria**	
	2018	**2019**	**2018**	**2019**	**2018**	**2019**	**2018**	**2019**
3.45−3.55 GHz	25.0	21.9	9.0	9.9	1.0	0.3	0.3	0.2
3.55−3.65 GHz	14.7	13.3	13.6	22.4	0.1	0.0	0.0	0.1

Figures 9 and 10 provide bar charts of mean band occupancy estimates for 3.45−3.55 GHz in 2018 and 2019, respectively. Light gray vertical bars indicate months when zero measurements were acquired. Months with no bar indicate that measurements were made and no signals were observed above the threshold.

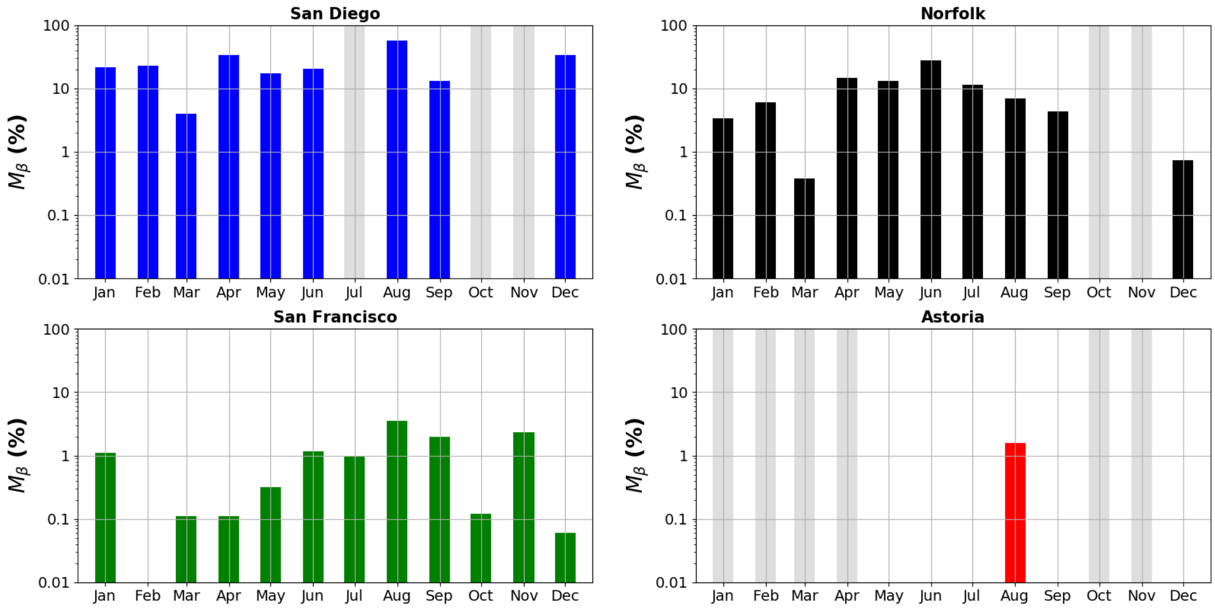

Figure 9. 2018 monthly mean band occupancy for 3.45−3.55 GHz at threshold L = -88 dBm.

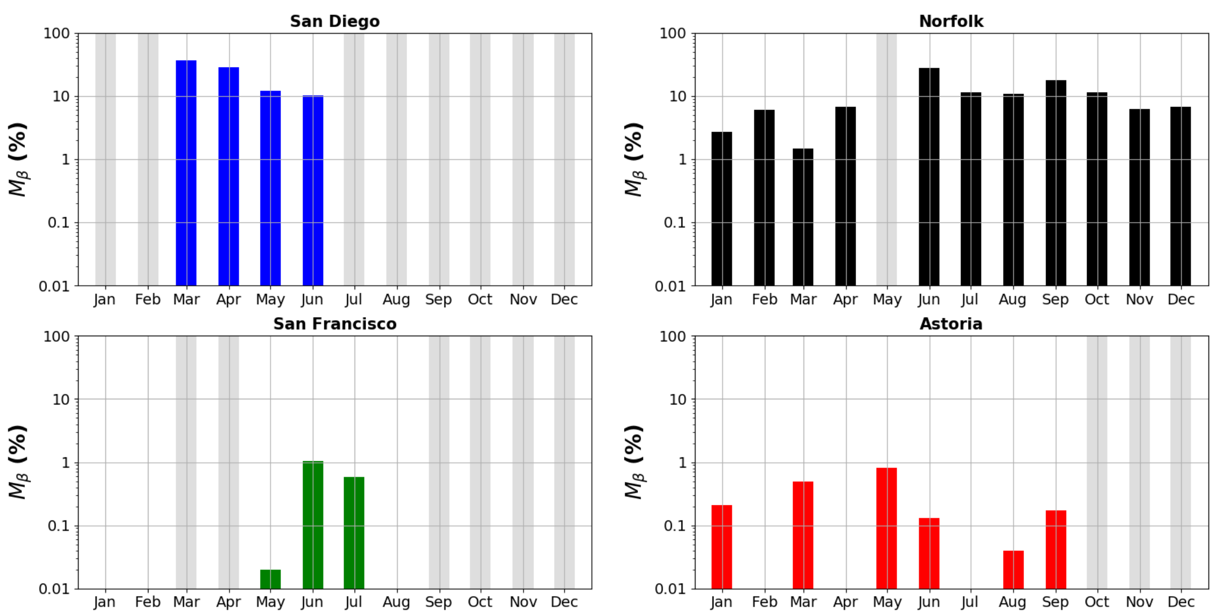

Figure 10. 2019 monthly mean band occupancy for 3.45−3.55 GHz at threshold L = -88 dBm.

Figures 11 and 12 provide bar charts of mean band occupancy estimates for 3.55−3.65 GHz in 2018 and 2019, respectively. Light gray vertical bars indicate months when zero measurements were acquired. Months with no bar indicate that measurement were made and no signals were observed above the threshold.

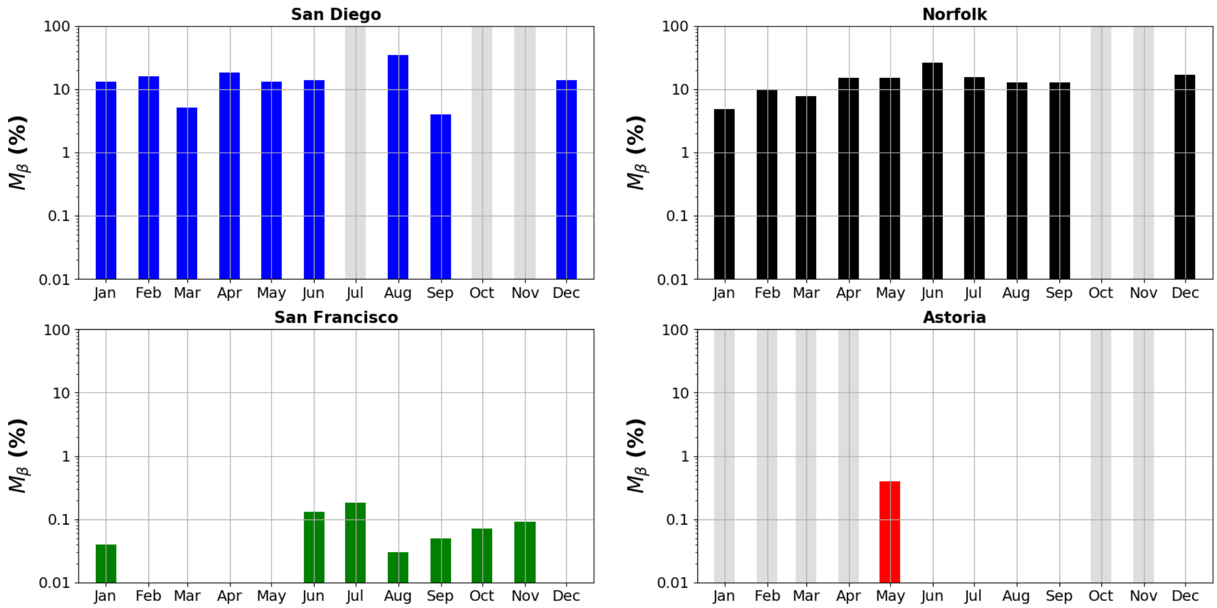

Figure 11. 2018 monthly mean band occupancy for 3.55−3.65 GHz at threshold L = -88 dBm.

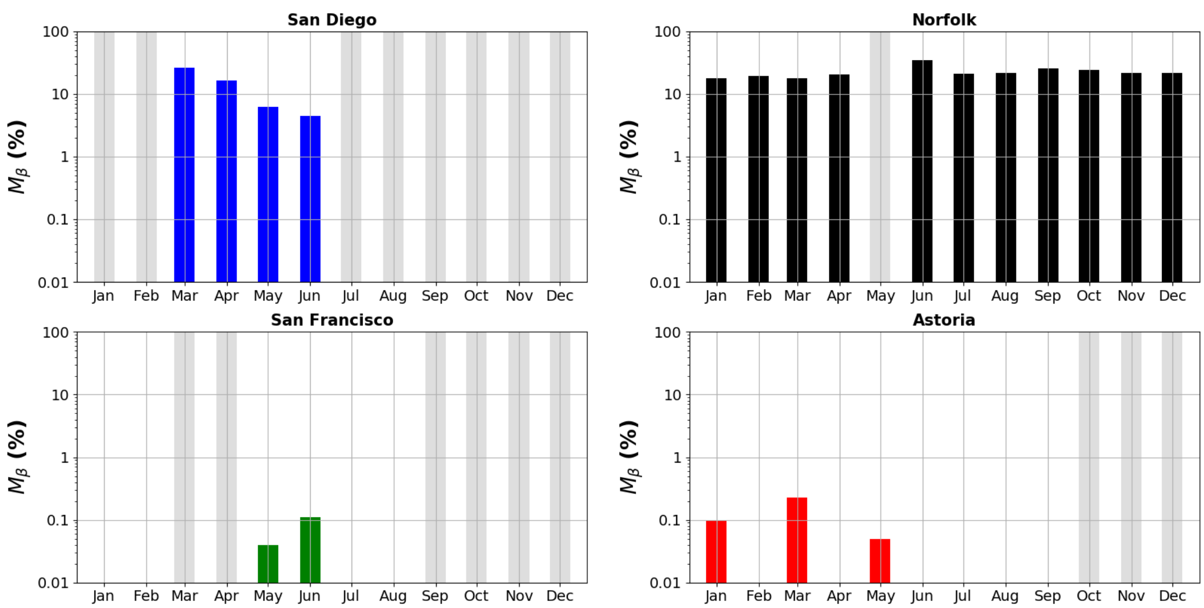

Figure 12. 2019 monthly mean band occupancy for 3.55−3.65 GHz at threshold L = -88 dBm.

5. SUMMARY

This report presents spectrum occupancy results for 3.45−3.55 GHz and 3.55−3.65 GHz at sensor sites near San Diego CA, Norfolk VA, San Francisco CA, and Astoria OR between January 2018 and December 2019. The goal of the measurement strategy was to perform continuous long-term measurements in order to provide factual occupancy information for 3.45−3.65 GHz emitters at and around the four locations. The sensor design (e.g., antenna selection, detection scheme) and installation (e.g., location, antenna configuration) are designed for detecting the SPN-43 air-marshalling radar that operates at 3.5−3.65 GHz and is a primary emitter in this band. There are other important ground-based, shipborne, and airborne government systems that operate in this frequency range. This approach is not necessarily optimal for detecting all 3.5 GHz government systems.

Non-zero occupancy was observed at all sites in both 2018 and 2019. Across the four sensor sites, the occupancy at San Diego was the highest. Referencing a -88 dBm threshold, mean band occupancy near San Diego in {2018, 2019} was estimated at {25.0, 21.9}% in the 3.45−3.55 GHz range and {14.7, 13.3}% in the 3.55−3.65 GHz range. Mean band occupancy near Norfolk was estimated at {9.0, 9.9}% in the 3.45−3.55 GHz range and {13.6, 22.4}% in the 3.55−3.65 GHz range. In contrast, less occupancy was observed at both the San Francisco and Astoria sites. Mean band occupancy near San Francisco was estimated at {1.0, 0.3}% in the 3.45−3.55 GHz range and {0.1, 0.0}% in the 3.55−3.65 GHz range. Mean band occupancy near Astoria was estimated at {0.3, 0.2}% in the 3.45−3.55 GHz range and {0.0, 0.1}% in the 3.55−3.65 GHz range.

6. REFERENCES

[1] Drocella E., R. Sole, and N. LaSorte, "Technical Feasibility of Sharing Federal Spectrum with Future Commercial Operations in the 3450−3550 MHz Band," NTIA Technical Report TR-20-546, U.S. Dept. of Commerce, Jan. 2020. https://www.ntia.doc.gov/report/2020/technical-feasibility-sharing-federal-spectrum-future-commercial-operations-3450-3550.

[2] Federal Communications Commission, "Amendment of the Commission's Rules with Regard to Commercial Operations in the 3550−3650 MHz Band" Report and Order and Second Further Notice of Proposed Rulemaking, 30 FCC Rcd 3959 (5), Apr. 2015, available at https://docs.fcc.gov/public/attachment/FCC-15-47A1.pdf.

[3] National Telecommunications and Information Administration, U.S. Dept. of Commerce, "Annual Report on the Status of Spectrum Repurposing," Aug. 2019. https://ntia.doc.gov/files/ntia/publications/spectrum-repurposing-report-august-2019.pdf.

[4] National Telecommunications and Information Administration, U.S. Dept. of Commerce, "An Assessment of the Near-Term Viability of Accommodating Wireless Broadband Systems in the 1675-1710 MHz, 1755-1780 MHz, 3500-3650 MHz, 4200-4220 MHz, and 4380-4400 MHz Bands (President's Spectrum Plan Report)," Oct. 2010. https://ntia.doc.gov/files/ntia/publications/fasttrackevaluation_1152010.pdf.

[5] Sanders F.H., J. E. Carroll, G. A. Sanders, J. S. Devereux and E. F. Drocella, "Procedures for Laboratory Testing of Environmental Sensing Capability Sensor Devices", NTIA Technical Report TR-18-527, U.S. Department of Commerce, Nov. 2017. http://www.its.bldrdoc.gov/publications/3184.aspx.

[6] Sanders F.H., R. L. Sole, G. A. Sanders and J. E. Carroll, "Further Procedures for Laboratory Testing of Environmental Sensing Capability Sensor Devices", NTIA Technical Memorandum TM-18-534, U.S. Department of Commerce, Jun. 2018. http://www.its.bldrdoc.gov/publications/3207.aspx.

[7] Cotton M. and R. Dalke, "Spectrum Occupancy Measurements of the 3550−3650 Megahertz Maritime Radar Band near San Diego, California," NTIA Technical Report TR-14-500, Jan. 2014. https://www.its.bldrdoc.gov/publications/2747.aspx.

[8] GNU Radio Foundation, "Signal Metadata Format Specification," v0.0.1, Jul. 17, 2018.

[9] National Telecommunications and Information Administration, U.S. Dept. of Commerce, "SigMF-NS-NTIA," v1.0.0, Mar. 5, 2020.

[10] Sanders F.H., J.E. Carroll, G.A. Sanders, and L.S. Cohen, "Measurements of Selected Naval Radar Emissions for Electromagnetic Compatibility Analyses," NTIA Report TR-15-510, Oct. 2014. https://www.its.bldrdoc.gov/publications/2781.aspx.

[11] MOBILE NOW Act, Pub. L, No. 115-141, Division P, Title VI, § 601 et seq. (2018).

APPENDIX A: METADATA

This appendix provides metadata examples from the San Diego sensor to define hardware, configuration, and algorithm. Metadata and data were packaged according to the gnuradio Signal Metadata Format Specification (SigMF) [8] and the SigMF-NS-NTIA extension [9]—i.e., NTIA's open data format for recorded signal datasets.


```
{
  "global" : {
    "core:datatype" : "rf32_le",
    "core:sample_rate" : 2.8E7,
    "core:version" : "v0.0.1",
    "core:description" : "Radar data captured off the coast of San
Diego",
    "core:extensions" : {
      "ntia-core" : "v1.0.0",
      "ntia-algorithm" : "v1.0.0",
      "ntia-sensor" : "v1.0.0",
      "ntia-environment" : "v1.0.0",
      "ntia-location" : "v1.0.0"
    },
    "ntia-sensor:sensor" : {
      "id" : "192.168.1.13",
      "sensor_spec" : {
        "id" : "bh-1",
        "model" : "bassethound",
        "version" : "v1.0.0",
        "description" : ""
      },
      "antenna" : {
        "antenna_spec" : {
          "model" : "ARA BSB-26",
          "description" : "RF antenna ideally suited for reception of
signals on the horizon for nautical and broadband surveillance
applications"
        },
        "type" : "Omni-directional",
        "frequency_low" : 2.0E9,
        "frequency_high" : 6.0E9,
        "gain" : 0.0,
        "polarization" : "slant",
        "cross_polar_discrimination" : 13.0,
        "horizontal_beam_width" : 360.0,
        "vertical_beam_width" : 68.38,
        "elevation_angle" : 0.0
        "voltage_standing_wave_ratio" : 2.0,
        "cable_loss" : 0.62,
        "steerable" : false,
      },
      "preselector" : {
        "cal_sources" : [ {
```

```
          "cal_source_spec" : {
            "id" : "36192",
            "model" : "Mercury Systems NS346B-1",
            "supplemental_information" :
"https://www.everythingrf.com/products/noise-sources/mercury-
systems/608-220-ns346b-1"
          },
          "type" : "Calibrated noise source",
          "enr" : "14.6 dB"
        } ],
        "filters" : [ {
          "filter_spec" : {
            "id" : "13FV40-00014, SN 7",
            "model" : "K&L 13FV40-3550/U200-o/o",
            "supplemental_information" :
"http://www.klfilterwizard.com/klfwpart.aspx?FWS=1112001&PN=13FV40-
3550%2fU200-O%2fO"
          },
          "frequency_low_passband" : 3.43E9,
          "frequency_high_passband" : 3.67E9,
          "frequency_low_stopband" : 3.39E9,
          "frequency_high_stopband" : 3.71E9
        }, { } ],
        "amplifiers" : [ {
          "amplifier_spec" : {
            "id" : "1904043",
            "model" : "MITEQ AFS3-02000400-30-25P-6",
            "supplemental_information" :
"https://nardamiteq.com/docs/MITEQ_Amplifier-AFS.JS_c41.pdf"
          },
          "gain" : 30.61,
          "noise_figure" : 2.76,
          "max_power" : 27.42
        } ],
        "rf_paths" : [ {
          "name" : "Path 1",
          "cal_source_id" : "36192",
          "filter_id" : "13FV40-00014, SN 7",
          "amplifier_id" : "1904043"
        }, {
          "name" : "Bypass",
          "cal_source_id" : "36192"
        } ]
      },
      "signal_analyzer" : {
        "sigan_spec" : {
          "id" : "US54230178",
          "model" : "Keysight N6841A",
          "supplemental_information" :
"https://www.keysight.com/us/en/assets/7018-02113/data-sheets/5990-
3839.pdf"
        },
```

```
        "frequency_low" : 2.0E7,
        "frequency_high" : 6.0E9,
        "noise_figure" : 20.0,
        "max_power" : 20.0,
        "a2d_bits" : 14
      },
      "computer_spec" : {
        "id" : "MC 5",
        "description" : "Custom computer with Intel i7 processor, MSI
motherboard, 16 GB of Ram and running Windows 7"
      },
      "location" : {
        "x" : xxx.xxxxx,
        "y" : yy.yyyyy,
        "z" : zzz.zzzzz,
        "speed" : 0.0,
        "description" : "Point Loma, near San Diego"
      },
      "environment" : {
        "category" : "Outside. Coastal"
      }
    },
    "ntia-location:coordinate_system" : {
      "coordinate_system_type" : "CoordinateSystem",
      "id" : "WGS84",
      "distance_unit" : "degree",
      "time_unit" : "second",
      "orientation_ref" : "IERS Reference Meridian",
      "elevation_ref" : "MSL",
      "elevation_unit" : "meter"
    },
    "ntia-sensor:calibration_datetime" : "2018-02-01T12:43:53.190Z",
    "ntia-core:measurement" : {
      "domain" : "Frequency",
      "measurement_type" : "Scan",
      "time_start" : "2018-02-01T07:59:58.553Z",
      "time_stop" : "2018-02-01T08:00:53.553Z",
      "frequency_tuned_low" : 3.45940625E9,
      "frequency_tuned_high" : 3.65190625E9,
      "frequency_tuned_step" : 1.925E7
    }
  },
  "captures" : [ {
    "core:sample_start" : 0,
    "core:frequency" : 3.5501875E9,
    "core:datetime" : "2018-02-01T07:59:58.553Z"
  } ],
  "annotations" : [ {
    "ntia-core:annotation_type" : "FrequencyDomainDetection",
    "core:sample_start" : 0,
    "core:sample_count" : 458,
    "core:comment" : "",
```

```
    "ntia-algorithm:detector" : "fft_max_power",
    "ntia-algorithm:number_of_ffts" : 2187500,
    "ntia-algorithm:number_of_samples_in_fft" : 64,
    "ntia-algorithm:window" : "Gauss-top",
    "ntia-algorithm:equivalent_noise_bandwidth" : 962500.0,
    "ntia-algorithm:frequency_start" : 3.45021875E9,
    "ntia-algorithm:frequency_stop" : 3.65015625E9,
    "ntia-algorithm:frequency_step" : 437500.0,
    "ntia-algorithm:reference" : "antenna terminal"
  }, {
    "ntia-core:annotation_type" : "CalibrationAnnotation",
    "core:sample_start" : 0,
    "core:sample_count" : 458,
    "core:comment" : " Calibration is done every 6 hours.",
    "ntia-sensor:gain_preselector" : 25.931,
    "ntia-sensor:noise_figure_sensor" : 9.892,
    "ntia-sensor:enbw_sensor" : 962500.000,
    "ntia-sensor:mean_noise_power_sensor" : -163.697,
    "ntia-sensor:mean_noise_power_units" : "dBm/Hz",
    "ntia-sensor:mean_noise_power_reference" : "antenna terminal",
    "ntia-sensor:temperature" : 18.556,
  }, {
    "ntia-core:annotation_type" : "SensorAnnotation",
    "core:sample_start" : 0,
    "core:sample_count" : 458,
    "ntia-sensor:rf_path_index" : 0,
    "ntia-sensor:overload" : false,
    "ntia-sensor:attenuation_setting_sigan" : 6.0
  } ]
}
```

APPENDIX B: SENSOR CONFIGURATION MANAGEMENT

Table B-1 provides a sensor configuration log.

Table B-1. Sensor configuration log.

Date	San Diego	Norfolk	San Francisco	Astoria
09/16	Hardware built	Hardware built	Hardware built	Hardware built
09/16−05/17	Laboratory calibration and test	Laboratory calibration and test	Laboratory calibration and test	Laboratory calibration and test
05/12/17	Install			
05/24/17		Install		
06/14/17	Measurement stop	Measurement stop		
07/17/17	Measurement start, new cal procedure	Measurement start, new cal procedure		
07/27/17			Install−problem	
08/24/17	Default SigAn atten = 0 dB			
09/21/17	Default SigAn atten = 3 dB			
11/14/17			Install complete—SigAn moved up to PS to resolve problem Default SigAn atten = 3 dB	
11/16/17	SigAn moved up to PS to improve performance			
02/05/18			Default SigAn atten = 0 dB	
05/31/18				Install
	06/29/18−08/02/18 Non-operational			
	09/30/18−12/03/18 12/11/18−03/12/19 Non-operational	09/21/18−12/06/18 Non-operational		09/22/18−12/03/18 Non-operational
		03/05/19−04/12/19 04/29/19−06/12/19 Non-operational	01/08/19−02/13/19 03/01/19−05/13/19 Non-operational	
03/12/19	Preselector replaced			
			08/02/19−Un-install Non-operational	
09/17/19	Start 700 MHz monitoring, stop 3.5 GHz monitoring.			
09/19/19				Un-install

ITS attempted to achieve continuous measurements over the two-year scope of this report. Sensor installation follows a standard procedure, e.g. (1) Determine RF cable between antenna and PS and measure loss—see Table 1; (2) Mount antenna, PS, and SigAn outside shelter; (3) Install measurement controller and cellular router inside shelter; (4) Run/Connect direct-current voltage and Ethernet cables from PS measurement controller; (5) Install directional antenna to improve the signal-to-noise ratio of cellular network connection; and (6) Perform short-term measurements to inform default SigAn attenuation setting. An uninterruptible power supply was used to mitigate power disruptions at the site.

The sensors are part of an official NTIA Federal Information Security Modernization Act (FISMA) Major Application named the NTIA Spectrum Monitoring System (SMS). Sensors were checked daily for operability, with automated testing of all the major components of the sensor. A summary report of these results was sent every morning to relevant staff for general system awareness, and to identify failures that could be rapidly addressed. A contingency plan was invoked when sensors were identified as unresponsive. Remediation times were variable and sometimes long, especially when travel to a remote site was required. Table B-2 provides percentage of time sensors were operational during 2018 and 2019.

Table B-2. Percentage of time sensors were operational during month.

Month	**2018**				**2019**			
	SD	**NF**	**SF**	**AS**	**SD**	**NF**	**SF**	**AS**
Jan	99.7	27.8	94.4		0.0	100.0	24.8	100.0
Feb	73.5	98.5	83.5		0.0	100.0	55.3	100.0
Mar	3.3	16.2	10.2		43.2	15.4	0.0	100.0
Apr	48.3	48.0	48.4		100.0	54.4	0.0	100.0
May	99.7	100.0	100.0	1.9	99.7	0.0	60.2	99.7
Jun	95.7	100.0	100.0	60.5	75.6	61.5	100.0	100.0
Jul	0.0	100.0	100.0	49.7	0.0	100.0	100.0	100.0
Aug	95.5	100.0	100.0	99.7	0.0	100.0	4.2	100.0
Sep	98.5	67.4	100.0	70.3	0.0	100.0	0.0	100.0
Oct	0.0	0.0	100.0	0.0		100.0	0.0	
Nov	0.0	0.0	100.0	0.0		100.0	0.0	
Dec	24.5	82.5	100.0	91.8		58.8	0.0	
Totals	53.2	61.7	86.4	46.7	35.4	74.2	28.7	100.0

APPENDIX C: INFORMATION FROM SENSORS BY MONTH

This appendix provides the number of scans (N), number and percentage of scans at overload (OL), and mean band occupancy (M_β) for each month in 2018 and 2019. Blank rows indicate that there were zero measurements performed that month.

Table C-1. Information by month from San Diego sensors, 2018.

Month	OL Information for 3.45−3.65 GHz			Monthly M_β (%) vs L (dBm) for 3.45−3.55 GHz				Monthly M_β (%) vs L (dBm) for 3.55−3.65 GHz			
	N	N_{OL}	%	-88	-80	-70	-60	-88	-80	-70	-60
Jan	39930	988	2.47	21.5	9.8	2.7	0.9	13.2	3.5	0.8	0.4
Feb	28236	300	1.06	22.9	9.4	2.3	0.9	16.1	4.3	0.3	0.2
Mar	1333	31	2.33	4.0	2.1	0.1	0.0	5.2	2.8	1.1	0.5
Apr	19186	413	2.15	34.2	20.7	10.6	5.0	18.5	6.2	1.5	0.6
May	38364	2157	5.62	17.4	10.0	5.0	3.1	13.1	5.8	1.4	0.7
Jun	38335	641	1.67	20.7	10.0	2.4	0.6	14.0	5.2	1.2	0.4
Jul											
Aug	35667	4580	12.84	57.3	42.7	29.0	19.4	34.9	13.3	2.2	1.0
Sep	40077	330	0.82	13.1	7.4	3.1	0.9	4.0	1.6	0.7	0.4
Oct											
Nov											
Dec	10540	217	2.06	33.8	20.2	13.2	6.8	13.7	3.0	0.0	0.0
Totals	251668	9657	3.45	25.0	14.7	7.6	4.2	14.7	5.1	1.0	0.5

Table C-2. Information by month from Norfolk sensors, 2018.

Month	OL Information for 3.45−3.65 GHz			Monthly M_β (%) vs L (dBm) for 3.45−3.55 GHz				Monthly M_β (%) vs L (dBm) for 3.55−3.65 GHz			
	N	N_{OL}	%	-88	-80	-70	-60	-88	-80	-70	-60
Jan	12335	13	0.11	3.4	0.8	0.0	0.0	4.8	0.3	0.1	0.0
Feb	39069	227	0.58	6.1	3.2	1.5	0.7	9.8	1.4	0.3	0.1
Mar	7226	2	0.03	0.4	0.1	0.0	0.0	7.6	0.1	0.0	0.0
Apr	19967	471	2.36	14.9	9.2	4.6	2.5	14.9	3.6	0.6	0.1
May	43327	897	2.07	13.1	7.8	4.1	2.1	15.2	3.1	0.7	0.2
Jun	41265	1123	2.72	27.9	17.6	8.8	3.7	26.2	7.8	1.6	0.4
Jul	44190	255	0.58	11.6	6.2	2.8	1.3	15.3	1.5	0.2	0.0
Aug	44135	153	0.35	7.0	2.9	1.2	0.3	12.8	0.9	0.2	0.1
Sep	28932	74	0.26	4.3	2.3	1.0	0.5	12.6	0.3	0.1	0.0
Oct											
Nov											
Dec	36683	55	0.15	0.7	0.3	0.1	0.0	16.9	0.1	0.0	0.0
Totals	317129	3270	0.92	9.0	5.0	2.4	1.1	13.6	1.9	0.4	0.1

Table C-3. Information by month from San Francisco sensors, 2018.

Month	OL Information for 3.45−3.65 GHz			Monthly M_β (%) vs L (dBm) for 3.45−3.55 GHz				Monthly M_β (%) vs L (dBm) for 3.55−3.65 GHz			
	N	N_{OL}	%	-88	-80	-70	-60	-88	-80	-70	-60
Jan	42093	0	0.00	1.1	0.8	0.4	0.1	0.0	0.0	0.0	0.0
Feb	33610	0	0.00	0.0	0.0	0.0	0.0	0.0	0.0	0.0	0.0
Mar	4542	0	0.00	0.0	0.0	0.0	0.0	0.0	0.0	0.0	0.0
Apr	20870	0	0.00	0.1	0.0	0.0	0.0	0.0	0.0	0.0	0.0
May	44591	0	0.00	0.3	0.1	0.0	0.0	0.0	0.0	0.0	0.0
Jun	43146	0	0.00	1.2	0.4	0.1	0.0	0.1	0.0	0.0	0.0
Jul	44585	0	0.00	1.0	0.3	0.0	0.0	0.2	0.0	0.0	0.0
Aug	44491	0	0.00	3.6	2.3	1.1	0.3	0.0	0.0	0.0	0.0
Sep	43061	9	0.02	2.0	0.9	0.2	0.0	0.0	0.0	0.0	0.0
Oct	44536	2	0.00	0.1	0.0	0.0	0.0	0.1	0.0	0.0	0.0
Nov	43085	1	0.00	2.3	1.6	0.8	0.2	0.1	0.0	0.0	0.0
Dec	44589	0	0.00	0.1	0.0	0.0	0.0	0.0	0.0	0.0	0.0
Totals	453199	12	0.00	1.0	0.5	0.2	0.1	0.1	0.0	0.0	0.0

Table C-4. Information by month from Astoria sensors, 2018.

Month	OL Information for 3.45−3.65 GHz			Monthly M_β (%) vs L (dBm) for 3.45−3.55 GHz				Monthly M_β (%) vs L (dBm) for 3.55−3.65 GHz			
	N	N_{OL}	%	-88	-80	-70	-60	-88	-80	-70	-60
Jan											
Feb											
Mar											
Apr											
May	734	0	0.00	0.0	0.0	0.0	0.0	0.0	0.0	0.0	0.0
Jun	26090	0	0.00	0.0	0.0	0.0	0.0	0.0	0.0	0.0	0.0
Jul	22145	0	0.00	0.0	0.0	0.0	0.0	0.0	0.0	0.0	0.0
Aug	44463	0	0.00	1.6	.9	0.4	0.1	0.0	0.0	0.0	0.0
Sep	30338	0	0.00	0.0	0.0	0.0	0.0	0.0	0.0	0.0	0.0
Oct											
Nov											
Dec	40931	0	0.00	0.0	0.0	0.0	0.0	0.0	0.0	0.0	0.0
Totals	164701	0	0.00	0.3	0.1	0.1	0.0	0.0	0.0	0.0	0.0

Table C-5. Information by month from San Diego sensors, 2019.

Month	**OL Information for 3.45−3.65 GHz**			**Monthly M_β (%) vs L (dBm) for 3.45−3.55 GHz**				**Monthly M_β (%) vs L (dBm) for 3.55−3.65 GHz**			
	N	**N_{OL}**	**%**	**-88**	**-80**	**-70**	**-60**	**-88**	**-80**	**-70**	**-60**
Jan											
Feb											
Mar	12620	1367	10.83	36.5	17.2	5.2	1.8	26.2	8.6	2.5	1.3
Apr	41209	729	1.77	28.9	17.4	5.6	1.7	16.4	6.2	0.5	0.1
May	42406	390	0.92	12.0	6.6	2.7	1.0	6.2	2.8	0.4	0.1
Jun	32395	114	0.35	10.3	6.5	2.6	0.7	4.5	1.5	0.2	0.0
Jul											
Aug											
Sep											
Oct											
Nov											
Dec											
Totals	128630	2600	3.47	21.9	11.9	4.0	1.3	13.3	4.8	0.9	0.4

Table C-6. Information by month from Norfolk sensors, 2019.

Month	**OL Information for 3.45−3.65 GHz**			**Monthly M_β (%) vs L (dBm) for 3.45−3.55 GHz**				**Monthly M_β (%) vs L (dBm) for 3.55−3.65 GHz**			
	N	**N_{OL}**	**%**	**-88**	**-80**	**-70**	**-60**	**-88**	**-80**	**-70**	**-60**
Jan	44540	27	0.03	2.7	1.6	0.6	0.1	18.1	0.9	0.1	0.0
Feb	39377	456	1.16	6.1	3.1	1.4	0.6	19.6	1.3	0.2	0.1
Mar	6747	42	0.62	1.5	0.7	0.2	0.1	18.0	0.9	0.2	0.1
Apr	23391	33	0.14	6.8	3.4	1.7	0.6	20.4	0.8	0.1	0.0
May											
Jun	26249	324	1.23	27.8	16.4	6.0	2.4	34.3	8.5	0.7	0.0
Jul	44332	226	0.51	11.4	6.8	3.2	1.2	20.9	0.9	0.1	0.0
Aug	44190	217	0.49	10.9	4.9	2.0	0.8	21.6	0.8	0.1	0.0
Sep	42249	588	1.39	17.8	9.5	3.8	1.6	25.5	2.6	0.4	0.1
Oct	44192	180	0.41	11.4	6.8	3.0	1.0	24.3	2.0	0.3	0.0
Nov	42863	135	0.31	6.2	3.5	1.9	0.8	22.0	0.9	0.3	0.1
Dec	25960	102	0.39	6.7	3.0	1.2	0.4	21.7	1.0	0.4	0.2
Totals	384090	2330	0.61	9.9	5.4	2.3	0.9	22.4	1.9	0.3	0.1

Table C-7. Information by month from San Francisco sensors, 2019.

Month	**OL Information for 3.45−3.65 GHz**			**Monthly M_β (%) vs L (dBm) for 3.45−3.55 GHz**				**Monthly M_β (%) vs L (dBm) for 3.55−3.65 GHz**			
	N	**N_{OL}**	**%**	**-88**	**-80**	**-70**	**-60**	**-88**	**-80**	**-70**	**-60**
Jan	11062	0	0.00	0.0	0.0	0.0	0.0	0.0	0.0	0.0	0.0
Feb	22290	0	0.00	0.0	0.0	0.0	0.0	0.0	0.0	0.0	0.0
Mar											
Apr											
May	26837	0	0.00	0.0	0.0	0.0	0.0	0.0	0.0	0.0	0.0
Jun	43150	0	0.00	1.1	0.6	0.2	0.0	0.1	0.0	0.0	0.0
Jul	44589	0	0.00	0.6	0.3	0.1	0.0	0.0	0.0	0.0	0.0
Aug	1866	0	0.00	0.0	0.0	0.0	0.0	0.0	0.0	0.0	0.0
Sep											
Oct											
Nov											
Dec											
Totals	149794	0	0.00	0.3	0.2	0.1	0.0	0.0	0.0	0.0	0.0

Table C-8. Information by month from Astoria sensors, 2019.

Month	**OL Information for 3.45−3.65 GHz**			**Monthly M_β (%) vs L (dBm) for 3.45−3.55 GHz**				**Monthly M_β (%) vs L (dBm) for 3.55−3.65 GHz**			
	N	**N_{OL}**	**%**	**-88**	**-80**	**-70**	**-60**	**-88**	**-80**	**-70**	**-60**
Jan	44595	0	0.00	0.2	0.1	0.0	0.0	0.1	0.0	0.0	0.0
Feb	40283	0	0.00	0.0	0.0	0.0	0.0	0.0	0.0	0.0	0.0
Mar	44537	0	0.00	0.5	0.1	0.0	0.0	0.2	0.0	0.0	0.0
Apr	43159	0	0.00	0.0	0.0	0.0	0.0	0.0	0.0	0.0	0.0
May	44471	0	0.00	0.8	0.4	0.1	0.0	0.0	0.0	0.0	0.0
Jun	43161	0	0.00	0.1	0.1	0.1	0.1	0.0	0.0	0.0	0.0
Jul	44592	0	0.00	0.3	0.1	0.0	0.0	0.1	0.0	0.0	0.0
Aug	44596	0	0.00	0.0	0.0	0.0	0.0	0.0	0.0	0.0	0.0
Sep	20767	0	0.00	0.2	0.1	0.0	0.0	0.0	0.0	0.0	0.0
Oct											
Nov											
Dec											
Totals	370161	0	0.00	0.2	0.1	0.0	0.0	0.1	0.0	0.0	0.0

NTIA FORM 29
(4-80)

U.S. DEPARTMENT OF COMMERCE
NATIONAL TELECOMMUNICATIONS AND INFORMATION ADMINISTRATION

BIBLIOGRAPHIC DATA SHEET

1. PUBLICATION NO. TR-20-548	2. Government Accession No.	3. Recipient's Accession No.
4. TITLE AND SUBTITLE 3.45–3.65 GHz Spectrum Occupancy from Long-Term Measurements in 2018 and 2019 at Four Coastal Sites		5. Publication Date April 2020 6. Performing Organization Code NTIA/ITS.T
7. AUTHOR(S) Michael Cotton, Linh Vu, Bradley Eales, and Adam Hicks		9. Project/Task/Work Unit No. 3161012-300
8. PERFORMING ORGANIZATION NAME AND ADDRESS Institute for Telecommunication Sciences National Telecommunications & Information Administration U.S. Department of Commerce 325 Broadway Boulder, CO 80305		10. Contract/Grant Number.
11. Sponsoring Organization Name and Address National Telecommunications & Information Administration Herbert C. Hoover Building 14th & Constitution Ave., NW Washington, DC 20230		12. Type of Report and Period Covered
14. SUPPLEMENTARY NOTES		

15. ABSTRACT (A 200-word or less factual summary of most significant information. If document includes a significant bibliography or literature survey, mention it here.)

This report presents spectrum occupancy results for 3.45–3.55 GHz and for 3.55−3.65 GHz at sensor sites near San Diego CA (SD), Norfolk VA (NF), San Francisco CA (SF), and Astoria OR (AS). Sensors operated at the following {start date, end date, 2018 reliability, 2019 reliability}: SD {05/17, 09/19, 53.2%, 35.4%}, NF {05/17, 12/19, 61.7%, 74.2%}, SF {11/17, 12/19, 86.4%, 28.7%}, AS {05/18, 09/19, 46.7%, 100.0%}. The acquired data was processed to monthly and yearly mean band occupancy estimates. At ports with high military presence,{2018, 2019} yearly mean band occupancy levels were {25.0, 21.9}% in SD and {9.0, 9.9}% in NF for 3.45−3.55 GHz and {14.7, 13.3}% in SD and {13.6, 22.4}% in NF for 3.55−3.65 GHz. At ports with low military presence, {2018, 2019} yearly mean band occupancy levels were {1.0, 0.3}% in SF and {0.3, 0.2}% in AS for 3.45−3.55 GHz and {0.1, 0.0}% in SF and {0.0, 0.1}% in AS for 3.55−3.65 GHz.

16. Key Words (Alphabetical order, separated by semicolons)

3450-3550 MHz, 3550-3650 MHz, Citizen Broadband Radio Service (CBRS), radar, spectrum monitoring, spectrum occupancy, spectrum sharing

17. AVAILABILITY STATEMENT ☒ UNLIMITED. ☐ FOR OFFICIAL DISTRIBUTION.	18. Security Class. (This report) Unclassified	20. Number of pages 37
	19. Security Class. (This page) Unclassified	21. Price:

NTIA FORMAL PUBLICATION SERIES

NTIA MONOGRAPH (MG)

A scholarly, professionally oriented publication dealing with state-of-the-art research or an authoritative treatment of a broad area. Expected to have long-lasting value.

NTIA SPECIAL PUBLICATION (SP)

Conference proceedings, bibliographies, selected speeches, course and instructional materials, directories, and major studies mandated by Congress.

NTIA REPORT (TR)

Important contributions to existing knowledge of less breadth than a monograph, such as results of completed projects and major activities.

JOINT NTIA/OTHER-AGENCY REPORT (JR)

This report receives both local NTIA and other agency review. Both agencies' logos and report series numbering appear on the cover.

NTIA SOFTWARE & DATA PRODUCTS (SD)

Software such as programs, test data, and sound/video files. This series can be used to transfer technology to U.S. industry.

NTIA HANDBOOK (HB)

Information pertaining to technical procedures, reference and data guides, and formal user's manuals that are expected to be pertinent for a long time.

NTIA TECHNICAL MEMORANDUM (TM)

Technical information typically of less breadth than an NTIA Report. The series includes data, preliminary project results, and information for a specific, limited audience.

For information about NTIA publications, contact the NTIA/ITS Technical Publications Office at 325 Broadway, Boulder, CO, 80305 Tel. (303) 497-3572 or e-mail ITSinfo@ntia.gov.